Characterization of Heterogeneous Distribution of Tumor Blood Flow in the Rat

Katsuyoshi Hori, Maroh Suzuki, Shigeru Tanda and Sachiko Saito

Department of Experimental Oncology, Research Institute for Tuberculosis and Cancer, Tohoku University, 4-1 Seiryo-machi, Aoba-ku, Sendai 980

Angioarchitectures of ascites hepatoma AH109A and Sato lung carcinoma (SLC) were quantitatively compared by measuring the following morphometric parameters: vascular density, vascular length, distance between tissues and their nearest blood vessel, and total length of microvascular network per unit area. When the vascular networks in these two types of tumors were compared in the initial stage, the morphological parameters were almost identical. Correlations between tumor size and the number of starting vessels and between enlargement of the tumor and the ensuing increase in pressure of the starting vessel were also evaluated with a microcomputer and an apparatus for measuring microvascular pressure. The total length of tumor vascular network to which one starting vessel supplied blood increased exponentially as the tumor increased in size exponentially. There was a positive correlation between tumor size and the number of starting vessels. The range of the blood supply from one starting vessel was evidently limited. The pressure of the starting vessel increased with enlargement of the tumor size. As soon as the pressure of the starting vessel reached a plateau, however, there was a rapid increase in low-flow or no-flow areas in regions within the tumor. From the results obtained, we consider that low-flow or no-flow areas, resistant to delivery of anticancer drugs, inevitably appear with the progression of tumor growth.

Key words: *In vivo* analysis — Tumor blood flow — Vascular structure — Starting vessel — No-flow area

Tumor blood flow is one of the important factors affecting the effectiveness of cancer chemotherapy.[1, 2] However, tumor blood flow is relatively small and there are considerable differences among the individual areas even within one tumor. The larger a tumor grows, the greater the inhomogeneity of tumor blood flow becomes and the more frequently low-flow areas or no-flow areas (areas where blood flow temporarily stops) appear within the tumor vascular network.[3-6] However, little is known about how and why low-flow and no-flow areas appear in tumors as they grow. To clarify the mechanism and the reason, we must determine the characteristics of tumor angioarchitecture and the function of the feeding vessel ("starting vessel"[7]) which supplies blood to the tumor vascular network.

The first purpose of the present research was to compare the architectures of the vascular networks of Yoshida rat ascites hepatoma AH109A and Sato lung carcinoma at the same vascularization stage. These two tumors are different from each other in character. The relevent morphometric parameters are vascular density, vascular length, distance between tissues and their nearest blood vessel, and total length of microvascular network per unit area. The second purpose was to clarify the functions of the starting vessel. For that purpose, we measured the total length of the vascular network from one starting vessel, analyzed the correlation between tumor size and the number of starting vessels, and measured the growth of the tumor vascular network and

ensuing change of starting vessel pressure. On the basis of these results, we discuss in this paper the reason why low-flow or no-flow areas, an important characteristic of tumor microcirculation, appear sporadically during tumor growth.

MATERIALS AND METHODS

Animal and tumors Male Donryu rats (Nippon Rat Co., Urawa) were used at 8–10 weeks of age and with an average weight of about 160–180 g. The tumors used were Yoshida rat ascites hepatoma AH109A, which has been maintained in our laboratory by successive intraperitoneal transplantation, and Sato lung carcinoma (SLC), maintained by subcutaneous transplantation.

Rat transparent chamber The chamber used in this experiment consists of a pair of quartz glass plates that cover the thin subcutaneous tissue of rat dorsum. Details of the chamber construction and surgical technique have been published elsewhere.[8] Briefly, aseptic surgical dissection of a 10 mm diameter hole was made in opposing surfaces of the dorsal flap. The skin was dissected away, leaving a thin subcutaneous tissue membrane. Then the chamber was inserted into the skin fold. When the entire operation was performed with practically no hemorrhage, recovery of the chamber area took place more rapidly than usual and a normal vascular network without inflammation could be observed. The mean thickness

of subcutaneous tissue within the transparent chamber was about $110\,\mu$m. The implanted piece of tumor (about 0.1 mm^3) grew in a sheet-like fashion within the chamber. **Observation and photography** A rat with the transparent chamber was anesthetized with an intramuscular injection of pentobarbital sodium (30 mg/kg) and placed on a heated stage at 34°C for microscopic observation. In the case of observations for many hours, anesthesia was maintained with enflurane (Ethrane; Abbott Laboratories, North Chicago, IL) using an anesthetic machine developed for small laboratory animals.[9] Inhalation anesthesia was a more satisfactory means of controlling the depth of narcosis for several hours. Observation and photography of the angioarchitecture in normal and tumor tissue within the chamber were carried out as described previously.[7]

Analyses of capillary networks in normal tissue and tumor Capillary networks in the normal tissue and the tumor were photographed at 400 × optical magnification (40 × objective, 10 × eyepiece). Individual photographs were assembled into a montage. A transparent vinyl sheet was placed over the photomontage. The blood vessels were traced by hand onto an overlay, and detailed microscopic observation was performed to distinguish between overlap of two vessels and ramification of a vessel. We could determine the complete architecture of the tumor microvascular network by using this technique.[7, 10] An example of a tracing of the vascular network in SLC is shown in Fig. 1A.

Parameters of 1) vascular density, 2) vessel length, 3) distance between tissues and their nearest blood vessel, and 4) total length of network per unit area were measured from the overlays of photomontages in order to compare quantitatively the microvascular network arrangement and the vessel geometry in normal tissue and the two different tumors. Although some of the parameters of angioarchitecture are not independent of each other, they are required to analyze the microhemodynamics of tumor vessels. Cumulative measuring area was 53 mm^2 in normal tissue (n=12), 49 mm^2 in AH109A (n=14) and 42 mm^2 in SLC (n=14). The stages of tumor vascularization which we analyzed were the first and the second stages according to Yamaura and Sato's classification,[11] in both AH109A and SLC.

1) Vascular density: Vascular density was measured according to Chalkley's method.[12] In practice, a transparent vinyl sheet on which 5 points were set was superimposed on the photomontage overlay and a point coincident with a blood vessel was counted as "one hit." Selection of areas was made by random movement of the vinyl sheet, and counts were followed until at least 500 hits were accumulated. The value of percent of the number of cumulative hits to the number of total points was calculated as vascular density.
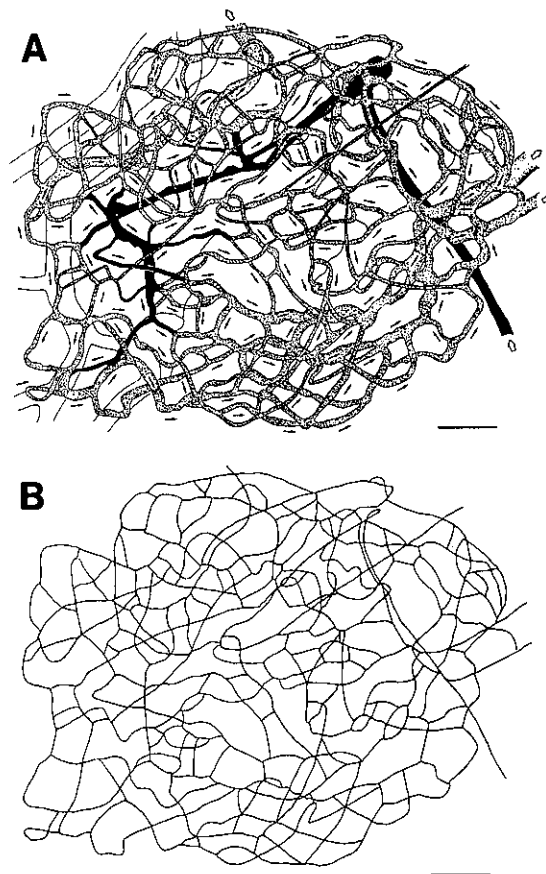

Fig. 1. (A) Overlay tracing of the photomontage of SLC tumor vascular network. The tumor vascular network was photographed at a 400 power magnification and individual photographs were assembled into a montage. A transparent vinyl sheet was placed over the photomontage and blood vessels were traced by hand onto an overlay. Blackened vessel: starting vessel. Shaded vessels: tumor capillaries. Arrows: flow direction. Bar scale: 100 μm. (B) Linearization of vascular network. The vascular network was linearized by drawing the center line of each vessel in the overlay tracing. Vascular length was measured by tracing the lines with a cursor interfaced with a digitizing tablet to a personal computer. Bar scale: 100 μm.

2) Vascular length: To measure vascular length, the line drawing of the photomontage (Fig. 1A) was linearized as shown in Fig. 1B. Vascular length, according to Skalak and Schmid-Schönbein,[13] was defined as the length of a vessel segment between two branching points. Vascular length was measured using a cursor interfaced with a digitizing tablet (WT-4400SE, WACOM Corporation, Saitama) to a personal computer (PC9801 VM4, NEC Corporation, Tokyo). Software used was Area-Distance Calculation Program (WACOM Corporation).

3) Distance between tissues and their nearest blood vessel: A transparent vinyl sheet on which one point was set was placed over the line drawing of photomontage and the shortest distance between the point defined and the nearest blood vessel was measured with a digitizer. Sites for measurement were selected by random movement of the vinyl sheet.

4) Total length of microvascular network per unit area: Total length of the microvascular network in an area of 0.045 mm^2 was measured in both normal subcutaneous tissues and tumors with a digitizer. Five or six different

Fig. 2. An example of pressure measurement in a starting vessel. (A) The pressure of microvessels was designated as 0 cm H$_2$O when the top of the needle was in contact with the vessel over the film membrane. (B) The pressure required for a temporary interruption of circulation was defined as the microvessel pressure. The pressure of the starting vessel designated with an arrow was 56.2 cm H$_2$O (41.3 mmHg). Blood flow through the tumor vascular network to which blood was supplied by the starting vessel completely stopped.

regions per chamber were selected. Measurements were taken in 133 regions in normal subcutis, 80 regions in AH109A and 38 regions in SLC.

Analyses of functions of "starting vessels" 1) Daily change in total length of a tumor vascular network supplied with blood by one starting vessel: We photographed the tumor vascular network of SLC to which one starting vessel supplied blood every 24 h, measuring the total length of the tumor vascular network.

2) Relationship between tumor size and number of starting vessels: SLC was used for this analysis, because it is easy to draw a definite line of demarcation between the tumor edge and normal tissue. Photographs were taken at a low magnification (objective 4×, ocular 10×) and individual prints were assembled into a montage. The number of starting vessels and the tumor size were correlated. The number of starting vessels entering a tumor was directly counted under the microscope at a magnification of 400 times. The size of the tumor was measured with a digitizer.

3) Pressure measurement of the starting vessel: Pressure in the starting vessel was measured by our micro-occlusion technique.[14] The structure of the transparent chamber for microvascular pressure measurement and the micropressure converter has been described previously.[14] Briefly, one side of the chamber has a window made of a quartz glass plate, and the other side has a ring covered with an 11 μm thick polyvinylidene chloride film membrane. A micromanipulator (ML-9; Narishige Scientific Instrument Lab. Co., Tokyo) was used to bring the top of the steel needle (SPRON 100; Sendai Seimitsu Material Res. Lab. Co. Ltd., Sendai) into contact with the under surface of the skin beneath the transparent chamber. The pressure required for a temporary interruption of circulation was defined as the microvessel pressure. One example of measuring pressure in the starting vessel by using this technique is shown in Fig. 2. The pressure in the starting vessel was measured periodically during tumor growth.

Statistical analysis Data were analyzed for significance by using Student's t test. The criterion of statistical significance was taken as $P < 0.05$.

RESULTS

Analysis of angioarchitecture in normal and tumor tissue
1) Vascular density: The average vascular density was 18 ±3% (range: 14–23%) in normal subcutis, 45±6% (range: 35–55%) in AH109A and 49±8% (range: 39–58%) in SLC. In terms of vascular density there was no significant difference between AH109A and SLC tumors.
2) Vascular length: The distributions of capillary length in normal subcutis and the two tumors are shown in Fig. 3. The median of capillary length in normal subcutis was
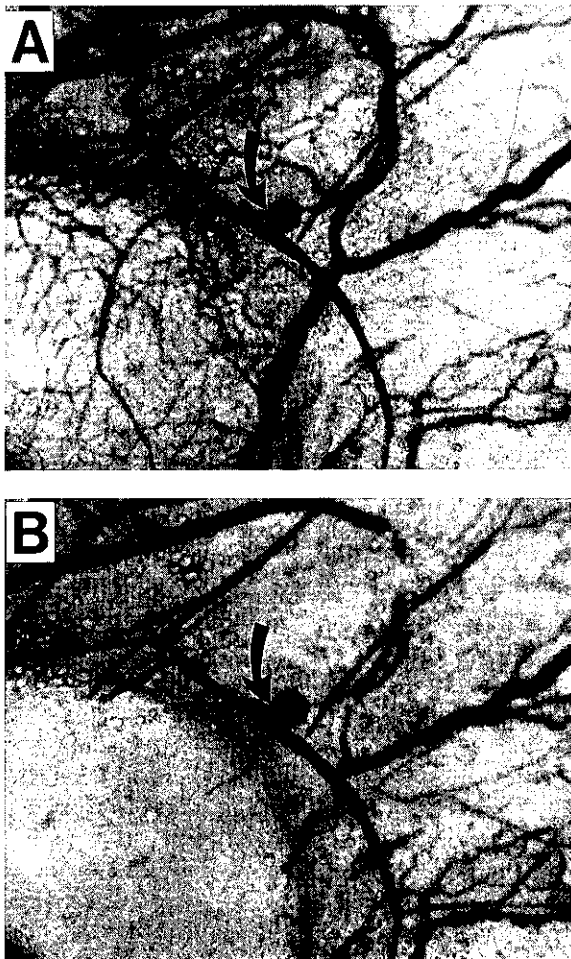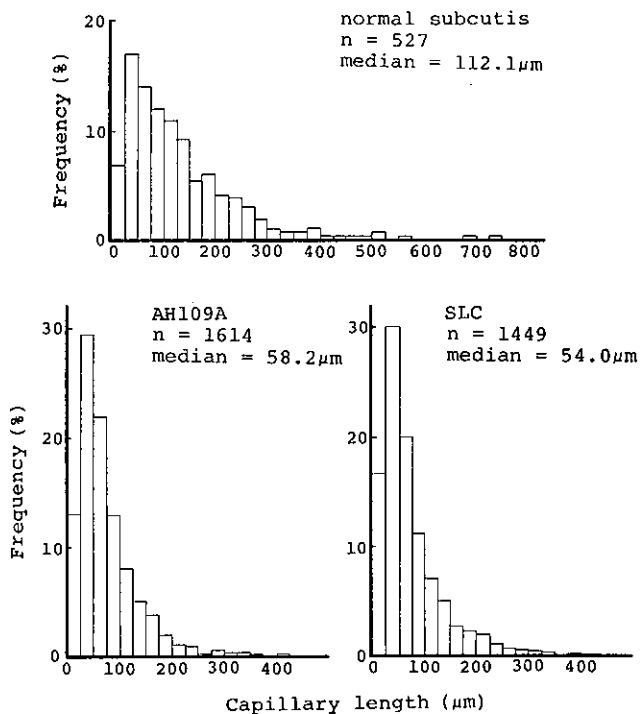
Fig. 3. Frequency distributions of the lengths of capillaries in normal subcutis and tumors (AH109A, SLC).
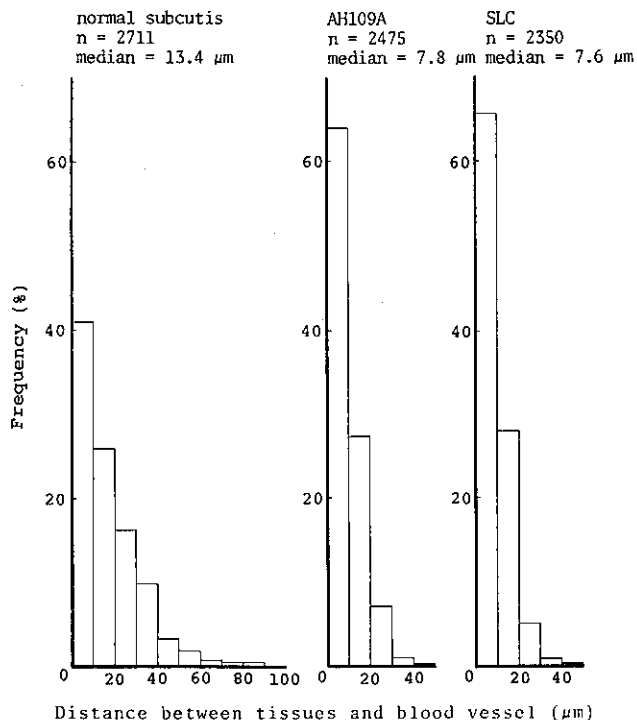

Fig. 4. Frequency distributions of the distance of tissues from blood vessel in normal subcutis and tumors (AH109A, SLC). n: number of samples.
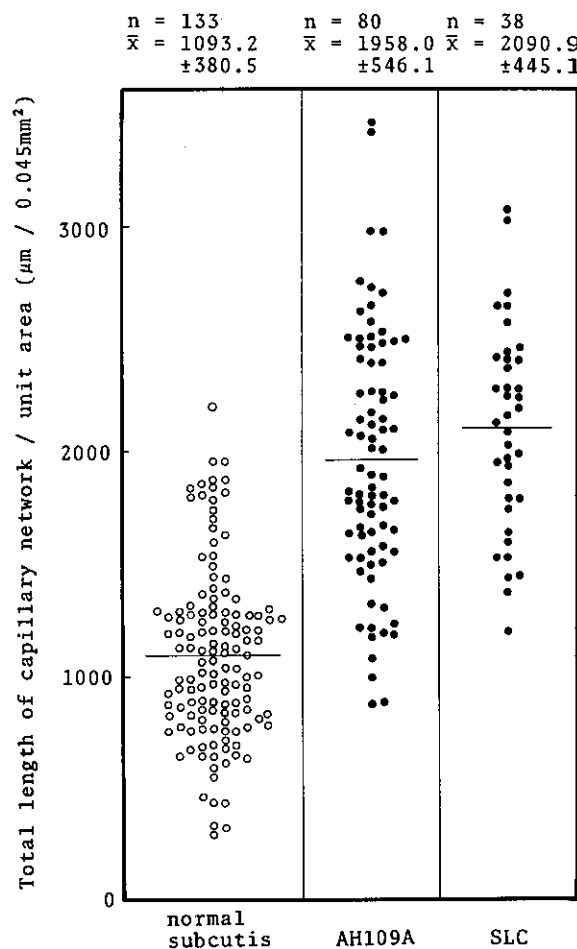

Fig. 5. Total length of microvascular network per unit area (0.045 mm^2).

112.1 μm (n=527). There were several vessels longer than 800 μm. Medians of capillary length in AH109A and SLC were 58.2 μm (n=1614) and 54.0 μm (n= 1449), respectively. Both the shape of the histograms and the median values indicate that the distributions of vascular length in the two tumors have almost the same pattern.

3) The distance between tissues and their nearest blood vessel: The distributions of the distance in normal subcutis and two tumors are shown in Fig. 4. Medians in the histograms for distance distribution in normal subcutis, AH109A, and SLC were 13.4 μm (n=2711), 7.8 μm (n=2475), and 7.6 μm (n=2350), respectively. The distance in normal subcutis was approximately twice as long as that in the tumors. The distribution of distance from tissues to blood vessels in the two tumors showed the same pattern.

4) Total length of microvascular network per unit area: The total length of microvascular network per unit area (0.045 mm²) in normal subcutis and the two tumors is indicated in Fig. 5. The average values of normal subcutis, AH109A, and SLC were 1093.2±380.5 µm (n=131), 1958.0±546.1 µm (n=80), and 2090.9±445.1 µm (n=38), respectively. The total length of vascular network per unit area in tumors was approximately twice as long as that of normal subcutis (P<0.001). However, there was no significant difference between AH109A and SLC (P>0.5).

Analyses of functions of the "starting vessel" 1) Daily change in total length of tumor vascular network with tumor growth: The total length of tumor vascular network increased exponentially as the tumor increased in size exponentially. The change in the vascular network of SLC at 24-h intervals is shown in Fig. 6. The total length of vascular network to which one starting vessel supplied blood was 7043.2 µm at the start of measurement, but reached 11365.6 µm, 16638.2 µm, and 25740.8 µm, respectively, after 24 h, 48 h and 72 h. Thus, the length increased by 3.7 times in 72 h.

2) Relationship between tumor size and number of starting vessels: The mean value of the tumor area at the time when new tumor vessels were first established was 2.4 mm² (range: 0.1–6.6 mm², n=28). The vascular network in the tumor microfoci within a transparent chamber usually consists of one starting vessel as an inflow and one or two outflow vessels. Tumor vascular networks whose blood flow was supplied by a starting vessel enlarged during tumor growth. When the tumor exceeded 2 mm in diameter, blood flow in some fields of the vascular network was supplied by a plural number of starting vessels (Fig. 7). As shown in Fig. 8, there was a positive
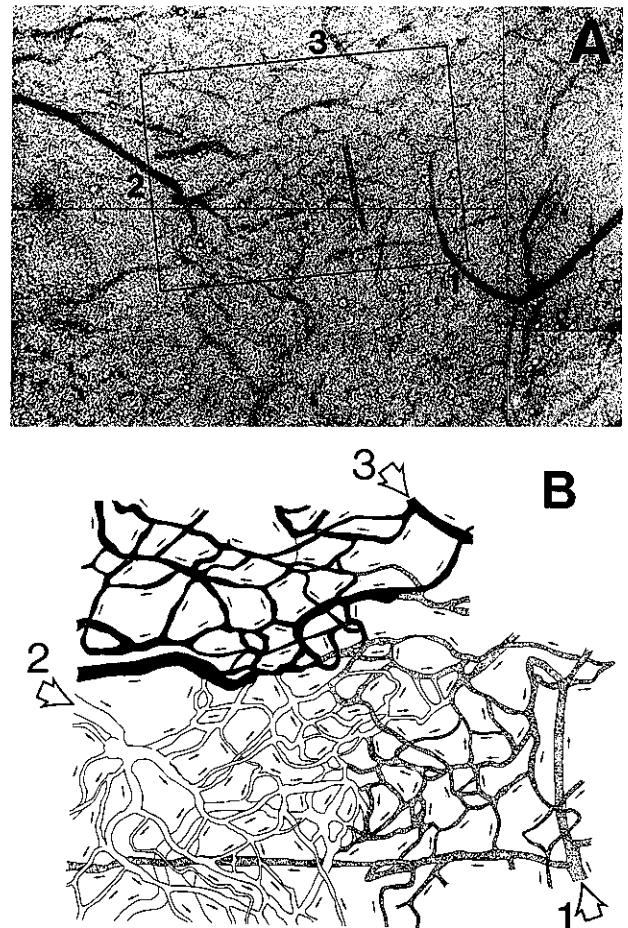
Fig. 7. Tumor vascular network to which 3 different starting vessels supplied blood. (A) Photograph of an SLC tumor vascular network (×40). Each starting vessel is numbered. (B) Overlay tracing of the photomontage (×400) of the SLC tumor vascular network in the square shown in (A). Each vascular network, in which blood flow is controlled by its own starting vessel, is indicated by the use of shaded, blackened and white vessels.
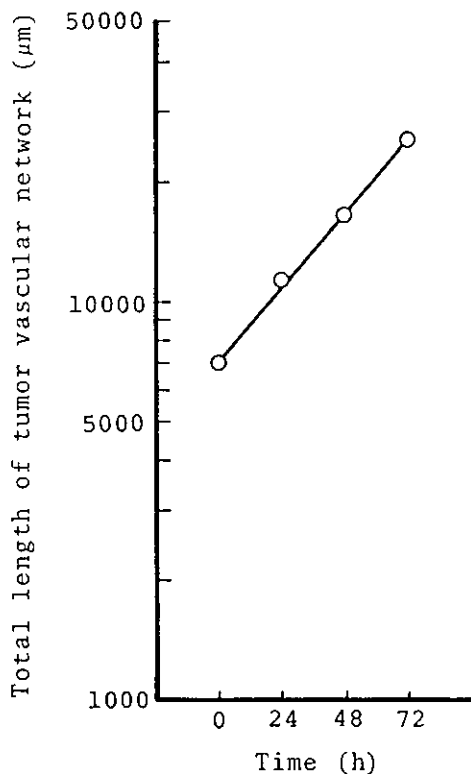

Fig. 6. Enlargement of vascular network of SLC at 24-h intervals. The total length of vascular network increased exponentially and increased by 3.7 times in the period of 72 h.
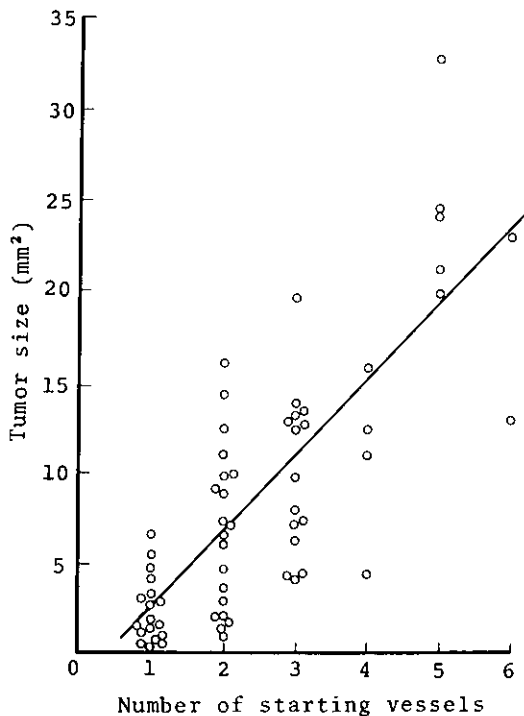
Fig. 8. Correlation between tumor size and the number of starting vessels. A highly significant correlation between the two parameters was observed in SLC [$y=4.1x-1.5$, $r=0.78$ ($P<0.001$), n=64].

correlation between tumor size and the number of starting vessels ($P<0.001$, n=64). The mean value of the tumor area under the control of one starting vessel was calculated as 4.1 mm^2 (n=64) from the slope of a regression line, as indicated in Fig. 8. The vascular network in large tumors was composed of many territories which were supplied with blood from different starting vessels. Tissue blood flow in each territory largely depended on the blood pressure of its own starting vessel. In one case, tumor blood flow within one territory was not observed for several hours (Fig. 9).

3) Change in pressure of the starting vessel with tumor growth: Pressure change in a given portion of a starting vessel is illustrated in Fig. 10. The pressure of the starting vessel was 41.3 cm H$_2$O (30.4 mmHg) at the initial stage of the neovascularization process. It became higher with increasing size of the tumor, and finally reached 126.0 cm H$_2$O (92.6 mmHg). The size of the tumor vascular network became larger as the pressure of its starting vessel increased. Even when the pressure of the starting vessel had reached a plateau, tumor vessels continued to grow for a period of time. Since the pressure of the starting vessel remained unchanged, the number of
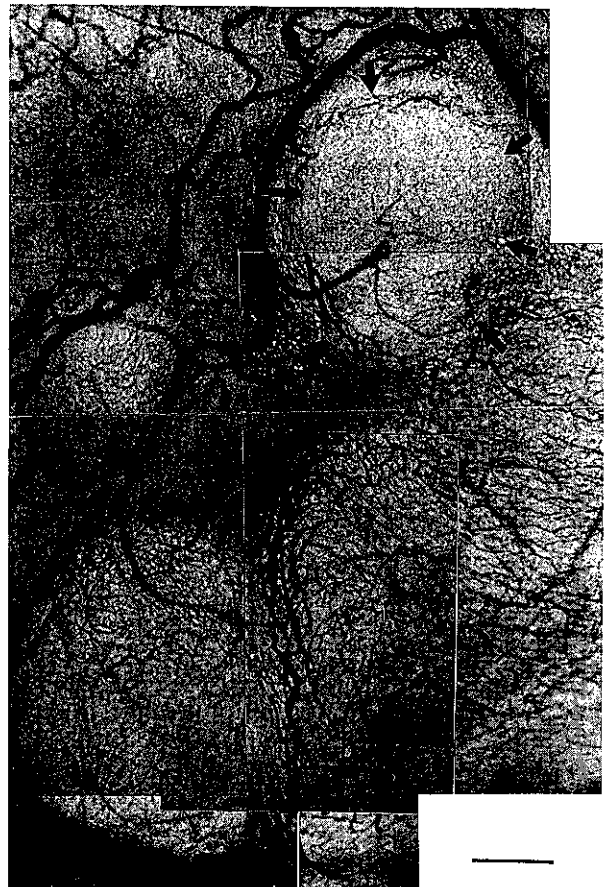

Fig. 9. Inhomogeneity of tumor blood flow. Tumor blood flow within one block (designated by arrows) remained stopped for several hours. Bar scale: 100 μm.

low-flow or no-flow areas, which looked as if they were avascular, increased rapidly.

DISCUSSION

Angioarchitecture in the initial stage of tumor growth In normal tissue, terminal arterioles are defined as the final arterial ramifications, and the branchings of these continue as nonmuscular capillary vessels.[15] We reported in a previous paper that the position from which tumor vessels originated was usually the terminal portion of a terminal arteriole, regardless of the kind of tumor.[7] In the first half of this paper we investigated whether or not there were angioarchitectures characteristic for each type of tumor.

Since Lewis[16] reported in 1927 that the vascular patterns of fibrosarcomas in rats were characteristic for each tumor type, there has been some debate as to whether or
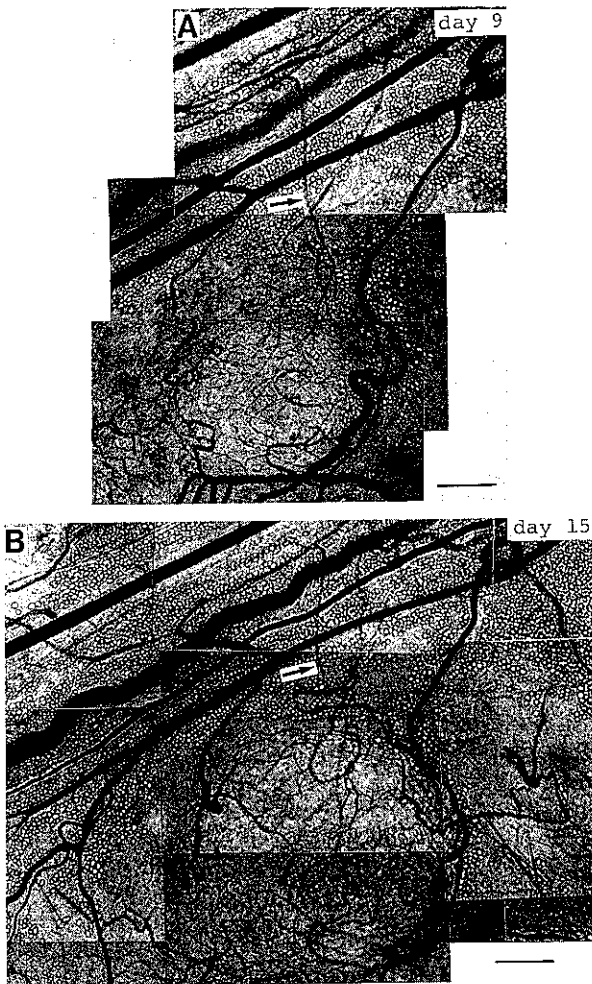
Fig. 10. Pressure elevation of a starting vessel in an identical location (designated by arrows). (A) vessel pressure: 41.3 cm H_2O (30.4 mmHg), tumor size: 1.23 mm^2, bar scale: 100 μm. (B) vessel pressure: 126.0 cm H_2O (92.6 mmHg), tumor size: 3.06 mm^2, bar scale: 100 μm.

not a tumor has its own vascular pattern.[17-22] By using a transparent chamber technique, Goodall et al.[17] showed that there were three main vascular patterns in tumors. Rubin and Casarett,[18] using the microangiographic method, and Falk,[19] using the resin injection method, reported two distinct tumor vascular patterns, that is, peripheral type and central type. On the other hand, Egawa et al.[20] reported that the vascular patterns of tumors were very similar, although four different tumor cell lines were examined. This controversy has arisen from comparing the vascular networks of different tumors without staging tumor vascularization. It is difficult to distinguish whether a difference of vascular pattern depends on the kind of tumor or on the stage of

the vascularization process, because tumor angioarchitecture changes markedly at different stages.

Tumor vessels, which are different from inflammation vessels, irreversibly become necrotic and never attain maturity.[23] Yamaura and Sato[11] observed the vascularization process of AH109A from initiation of angiogenesis to necrosis and divided the process into 4 stages based on changes in vascular morphology and vascular volume. Changes in vascular volume in each stage may be summarized as follows. In normal subcutaneous tissue, vascular volume remains at 20% of the tissue. When the tumor is implanted onto this subcutaneous tissue, the volume of tumor capillaries increases significantly. From the first to the second stages, the frequency of branching point formation increases and most tumor capillaries are elongated and dilated. Late in the second stage, the vascular volume finally reaches 50%. Late in the third stage and in the fourth stage, this value decreases rapidly to zero.

The time elapsed from the initiation of tumor vessel formation to necrosis depends on the kind of tumor. However, the process of vascularization in AH109A tumor reported by Yamaura and Sato[11] is similar to that observed in SLC and AH272 (Hori et al., unpublished data). To determine whether angioarchitectures are characteristic for each type of tumor, the tumors must be compared at the same stage. We compared the angioarchitecture in AH109A with that in SLC at the same stages of vascularization. Stages selected for analysis were the first stage and the second stage, in which vascular length in the tumor was about half that of normal subcutaneous tissue. The distance between a vessel and tissues became markedly shorter in these stages. When the vascularization stages in AH109A and in SLC were identical, the morphological parameters of the vascular network, that is, vascular density, vascular length, and the distance between tissues and a vessel were too similar to allow distinction between the two tumors.

From the facts that the positions where tumor vessels originated were identical and that the morphological parameters in the initial stage were also identical, we believe that the mode of tumor vascularization in the initial stage is similar, regardless of the kind of tumor. **The functions of the "starting vessel"** Terminal arterioles also changed in shape during tumor vascularization, and the structure and function of the modified terminal arterioles were different from those of normal ones. We refer to the terminal arteriole involved in the tumor as the "starting vessel" for initiation of tumor angiogenesis.[7]

In the present study, we found that a capillary network from one starting vessel turned into a tumor microvascular network unit. Many starting vessels ran into one large tumor. Each starting vessel controlled the blood

flow of its own territory. In general, the stage of tumor vascularization differed slightly from that of others in each territory. This is the reason why vessel morphology and tissue blood flow vary according to the location within a tumor.

The total length of the tumor vascular network in the territory increased exponentially when the tumor was growing exponentially. Finally, the total length of the vascular network became several times as long as that in the initial state. Increase of the vascular length creates resistance to blood flow. If the pressure of the starting vessel did not change in spite of the increase in the total vascular length, blood flow in each tumor vessel would drop precipitously. In reality, however, the larger the vascular network became, the higher the pressure of the starting vessel became in the initial state.

Suzuki et al.[24] and Yaegashi and Takahashi[25] reported that the medial smooth muscle of host arteries involved in tumors degenerated completely. There is no doubt that the regression of smooth muscle changes a terminal arteriole into a passive vessel (starting vessel). As a matter of course, blood which should naturally flow into a normal arteriole passes into the starting vessel. The pressure elevation of the starting vessel with tumor growth is perhaps caused by the increased flow of blood through the vessel. In fact, as soon as the pressure of the terminal arteriole began to increase, the contractile reaction of the terminal arteriole to angiotensinII was lost (Hori et al., unpublished data).

Why do low-flow and no-flow vessels appear within a tumor? In the first and the second stages, vascular density in the tumor became much higher than that in normal tissue. It has been reported that vascular permeability in tumors is higher than that in normal tissues.[26, 27] Therefore, while a tumor remains in the state of microfoci, drug delivery to the tumor tissues is not at all inferior to that to normal tissue. However, areas growing under such conditions exist only in very limited regions and times within the tumor.

By analyzing the correlation between the number of starting vessels and tumor areas fed by the vessel, we found that the range of the blood supply from one starting vessel was limited. When pressure elevation of a starting vessel reached a plateau, not all tumor vessels could sustain active flow simultaneously, only some vessels being perfused at one time. The regression of tumor vessels was associated with the stoppage or absence of circulation. We concluded that low-flow and no-flow areas were produced by the imbalance between the pressure elevation of a starting vessel and the enlargement of the vascular network from that vessel.

We also reported in the previous paper that the pressure of the tumor vessel was lower than that of normal vessels and gradually decreased with tumor growth.[28] This result might be explained by the fact that each tumor vessel moves gradually away from the starting vessel with tumor growth. We often observed that one territory next to a well-perfused territory had no blood flow. We proved in another experiment that this stoppage of blood flow was temporary and blood recirculated within a few hours.[29] This stoppage of blood flow within one territory seemed to be due to a temporary increase in local tissue pressure near that territory.

From the results mentioned above, we believed that regardless of the type of tumor, the vascularization process in tumors is similar and that appearance of low-flow or no-flow areas is an inevitable consequence of a very specialized tumor vascularization. Such low-flow or no-flow areas might be inaccessible to anticancer drugs, which might explain the poor results of conventional cancer chemotherapy in such cases.

The pressure of a starting vessel is elevated by angiotensinII-induced hypertension.[30] In turn, the elevated pressure of the starting vessel brought about a marked increase in tumor blood flow,[31, 32] affecting blood flow in the no-flow areas.[33] We will report in detail the mechanism of several-fold increases in tumor blood flow by angiotensinII in a separate paper.

ACKNOWLEDGMENTS

REFERENCES

1) Suzuki, M., Hori, K., Abe, I., Saito, S. and Sato, H. Functional characterization of the microcirculation in tumors. *Cancer Metastasis Rev.*, **3**, 115–126 (1984).

2) Jain, R. K. Determinants of tumor blood flow: a review. *Cancer Res.*, **48**, 2641–2658 (1988).

3) Brown, J. M. Evidence for acutely hypoxic cells in mouse tumours, and a possible mechanism of reoxygenation. *Br. J. Radiol.*, **52**, 650–656 (1979).

4) Hori, K., Suzuki, M., Abe, I., Saito, S. and Sato, H. Increase in tumor microvascular pressure by angiotensin-induced hypertension: implication for pharmacokinetic analysis of drug delivery into tumor tissue. *Jpn. J. Cancer*

Chemother., **10**, 953–960 (1983) (in Japanese).

5) Ackerman, N. B. and Makohon, S. The blood supply of experimental liver metastasis. VII. Further studies on increased tumor vascularity caused by epinephrine. *Microcirc. Endothelium Lymphatics,* **1**, 547–568 (1984).

6) Chaplin, D. J., Durand, R. E. and Olive, P. L. Acute hypoxia in tumors: implications for modifiers of radiation effects. *Int. J. Radiat. Oncol. Biol. Phys.,* **12**, 1279–1282 (1986).

7) Hori, K., Suzuki, M., Tanda, S. and Saito, S. *In vivo* analysis of tumor vascularization in the rat. *Jpn. J. Cancer Res.,* **81**, 279–288 (1990).

8) Hori, K., Suzuki, M., Abe, I. and Saito, S. Rat transparent chamber techniques for morphological and functional analysis in microcirculation. *Kokenshi,* **37**, 269–278 (1985) (in Japanese).

9) Hori, K., Suzuki, M., Saito, S., Tanda, S., Li, Y. and Zhang, Q. H. A new anesthetic machine for small laboratory animals. *Kokenshi,* **40**, 305–310 (1988) (in Japanese).

10) Engelson, E. T., Schmid-Schönbein, G. W. and Zweifach, B. W. The microvasculature in skeletal muscle II. Arteriolar network anatomy in normotensive and spontaneously hypertensive rats. *Microvasc. Res.,* **31**, 356–374 (1986).

11) Yamaura, H. and Sato, H. Quantitative studies on the developing vascular system of rat hepatoma. *J. Natl. Cancer Inst.,* **53**, 1229–1240 (1974).

12) Chalkley, H. W. Method for quantitative morphologic analysis of tissue. *J. Natl. Cancer Inst.,* **4**, 47–53 (1943).

13) Skalak, T. C. and Schmid-Schönbein, G. W. The microvasculature in skeletal muscle IV. A model of the capillary network. *Microvasc. Res.,* **32**, 333–347 (1986).

14) Hori, K., Suzuki, M., Abe, I., Saito, S. and Sato, H. A micro-occlusion technique for measurement of the microvascular pressure in tumor and subcutis. *Gann,* **74**, 122–127 (1983).

15) Wiedeman, M. P. Architecture. *Handb. Physiol. Sect. 2: Cardiovasc. Syst.,* **4**, 11–40 (1984).

16) Lewis, W. H. The vascular pattern of tumors. *Bull. Johns Hopkins Hosp.,* **41**, 156–162 (1927).

17) Goodall, C. M., Sanders, A. G. and Shubik, P. Studies of vascular patterns in living tumors with a transparent chamber inserted in hamster cheek pouch. *J. Natl. Cancer Inst.,* **35**, 497–521 (1965).

18) Rubin, P. and Casarett, G. Microcirculation of tumors. Part I: Anatomy, function, and necrosis. *Clin. Radiol.,* **17**, 220–229 (1966).

19) Falk, P. Patterns of vasculature in two pairs of related fibrosarcomas in the rat and their relation to tumour responses to single large doses of radiation. *Eur. J. Cancer,* **14**, 237–250 (1978).

20) Egawa, J., Ishioka, K. and Ogata, T. Vascular structure of experimental tumours. *Acta Radiol. Oncol.,* **18**, 367–375 (1979).

21) Gabbert, H., Wagner, R. and Hohn, P. The relation between tumor cell proliferation and vascularization in differentiated and undifferentiated colon carcinomas in the rat. *Virchows Arch. (Cell. Pathol.),* **41**, 119–131 (1982).

22) Solesvik, O. V., Rofstad, E. K. and Brustad, T. Vascular structure of five human malignant melanomas grown in athymic nude mice. *Br. J. Cancer,* **46**, 557–567 (1982).

23) Algire, G. H. and Chalkley, H. W. Vascular reactions of normal and malignant tissues *in vivo*. I. Vascular reactions of mice to wounds and to normal and neoplastic transplants. *J. Natl. Cancer Inst.,* **6**, 73–85 (1945).

24) Suzuki, M., Takahashi, T. and Sato, T. The medial regression in tumor-bearing host arteries and its functional significance: a morphometric study of hepatic arteries in human livers with hepatocellular carcinomas. *Cancer,* **59**, 444–450 (1987).

25) Yaegashi, H. and Takahashi, T. Encasement and other deformations of tumor-embedded host arteries due to loss of medial smooth muscle. Morphometric and three-dimensional reconstruction studies on some human carcinomas. *Cancer,* **65**, 1097–1103 (1990).

26) Nugent, L. J. and Jain, R. K. Extravascular diffusion in normal and neoplastic tissues. *Cancer Res.,* **44**, 238–244 (1984).

27) Heuser, L. S. and Miller, F. N. Differential macromolecular leakage from the vasculature of tumors. *Cancer,* **57**, 461–464 (1986).

28) Hori, K., Suzuki, M., Abe, S. and Saito, S. Changes in tumor transvascular pressure difference associated with tumor growth: implications for angiotensin-induced hypertension chemotherapy. *Jpn. J. Cancer Chemother.,* **12**, 1630–1637 (1985) (in Japanese).

29) Hori, K., Suzuki, M., Saito, S., Tanda, S. and Zhang, Q. H. Fluctuation of tumor blood flow under normotension; implication for induced hypertension chemotherapy. *Proc. Jpn. Cancer Assoc., 47th Annu. Meet.,* 550 (1988) (in Japanese).

30) Hori, K., Suzuki, M., Saito, S. and Tanda, S. Development of the angioarchitecture and microcirculatory characteristics in rat tumor. *Jpn. J. Cancer Chemother.,* **17**, 554–563 (1990) (in Japanese).

31) Suzuki, M., Hori, K., Abe, I., Saito, S. and Sato, H. Characteristic blood circulation in tumor tissue, with reference to cancer chemotherapy. *Jpn. J. Cancer Chemother.,* **5**, 77–80 (1978) (in Japanese).

32) Suzuki, M., Hori, K., Abe, I., Saito, S. and Sato, H. A new approach to cancer chemotherapy. Selective enhancement of tumor blood flow with angiotensin II. *J. Natl. Cancer Inst.,* **67**, 663–669 (1981).

33) Hori, K., Suzuki, M., Abe, I., Saito, S. and Sato, H. Increase in tumor vascular area due to increased blood flow by angiotensin II in rats. *J. Natl. Cancer Inst.,* **74**, 453–459 (1985).